PARAMETERS OF HIGH-TEMPERATURE RELAXATION SPECTRUM IN A METAL

S. I. Meshkov and A. S. Podkopaev

UDC 532.135 + 539.67

1. The monotonic growth of internal relaxation friction as the temperature rises or the vibration frequency diminishes is customarily designated background.

Within the framework of the one-dimensional linear theory of viscoelasticity for the Abel and A. R. Rzhanitsyn aftereffect kernels, as well as any Yu. N. Rabotnov kernels, any assumption about the complete relaxation of the elastic modulus will result in the following dependence of the internal friction background on frequency:

$$\operatorname{tg}\delta = \sin\psi/((\omega\tau)^{\gamma} + \cos\psi),\ \psi \equiv \pi\gamma/2,\ 0 < \gamma \leqslant 1, \tag{1.1}$$

where $\tan\delta$ is the loss angle tangent, ω is the cyclic vibrations frequency, τ is the relaxation time, γ is the divisibility parameter characterizing the spreading of the relaxation spectrum [1]. Moreover, if the Abel aftereffect kernel and the corresponding Yu. N. Rabotnov relaxation resolvent kernel are used then the frequency dependence of the background can be described without assuming complete relaxation of the shear modulus. Then the formula [2]

$$\operatorname{tg}\delta = \sin\psi/(\nu^{-1}(\omega\tau)^{\gamma} + \cos\psi),\ \nu \equiv (\mu_u - \mu_r)/\mu_u. \tag{1.2}$$

is obtained for the internal friction. Here μ_u and μ_r are the unrelaxed and relaxed values of the shear modulus.

Besides the methods in which dynamic shear loads are applied to the specimen, methods of longitudinal and bending vibrations in which the specimen experiences tension-compression deformations are used extensively in experiment. Let us write the expression for the internal friction in this case.

Let the complex shear modulus μ^* be described by a generalized Maxwell model:

$$\mu^* = \mu_u(i\omega\tau)^{\gamma}/(1 + (i\omega\tau)^{\gamma}). \tag{1.3}$$

The complex Young's modulus E^* is expressed in terms of the shear modulus μ^* and the multilateral compression K whose relaxation is ordinarily considered negligible:

$$1/E^* = 1/3\mu^* + 1/9K. \tag{1.4}$$

An expression for the real and imaginary parts of the complex pliability J^* and the internal friction under tension-compression vibrations follows from (1.3) and (1.4)

$$\operatorname{Re} J^* = \frac{3}{3\mu_u}\left[1 + \frac{\cos\psi}{(\omega\tau)^{\gamma}}\right] + \frac{1}{9K},\quad \operatorname{Im} J^* = -\frac{1}{3\mu_u}\frac{\sin\psi}{(\omega\tau)^{\gamma}}; \tag{1.5}$$

$$\operatorname{tg}\delta = -\operatorname{Im}J^*/\operatorname{Re}J^* = \sin\psi/[(1 + \mu_u/3K)(\omega\tau)^{\gamma} + \cos\psi]. \tag{1.6}$$

The last expression differs from (1.1) only by the coefficient of the quantity $(\omega\tau)^{\gamma}$.

According to (1.5), a relationship

$$\operatorname{Im} J^* = -\operatorname{tg}\psi(\operatorname{Re} J^* - (3K + \mu_u)/(9K\mu_u)) = -\operatorname{tg}\psi(\operatorname{Re} J^* - 1/E_u),$$
$$E_u \equiv 9K\mu_u/(3K + \mu_u)$$

Moscow. Kuibyshev. Translated from Zhurnal Prikladnoi Mekhaniki i Tekhnicheskoi Fiziki, No. 3, pp. 120-124, May-June, 1984. Original article submitted May 13, 1983.

0021-8944/84/2503-0447$08.50

exists between the imaginary and real parts of the pliability J*. Therefore, we have the equation of a line that intersects the abscissa axis at the point $1/E_u$ at an angle $2\pi - \pi\gamma/2$ measured in the positive direction in the plane of the complex pliability.

The equation of a circle with center at the point $\mathrm{Re}\, E^* = E_u/2$, $\mathrm{Im}\, E^* = -(E_u \cot \psi)/2$ passing through the origin

$$\left(\mathrm{Re}\, E^* - \frac{E_u}{2}\right)^2 + \left(\mathrm{Im}\, E^* + \frac{E_u}{2} \operatorname{ctg} \psi\right)^2 = \left(\frac{E_u}{2} \operatorname{cosec} \psi\right)^2 \tag{1.7}$$

is obtained in the plane of the complex modulus.

The argument of the expressions governing the dissipative and elastic characteristics in linear viscoelasticity theory is the dimensionless quantity $\omega\tau$. The temperature dependence of the relaxation time τ is customarily described by the Arrhenius formula

$$\tau = \tau_0 \exp(U/RT), \tag{1.8}$$

where U is the activation energy of the relaxation process, τ_0 is the characteristic relaxation time, and R is the universal gas constant.

Therefore, two possibilities exist for changing the quantity $\omega\tau$: a direct change in the frequency for a constant specimen temperature or heating at a constant frequency. The increase in frequency is here equivalent to a diminution in the temperature and vice versa. This property of relaxation processes is called the temperature–frequency equivalence.

Using the Arrhenius formula, we write an expression for the initial section of the temperature–frequency dependence of the internal friction background when the quantity $\cos \psi$ in the denominator of (1.1), (1.2), and (1.6) can be neglected

$$\operatorname{tg} \delta = C_i \omega^{-\gamma} \exp(-\gamma U/RT), \quad i = 1, 2, 3, \tag{1.9}$$
$$C_1 = \sin \psi/\tau^\gamma, \quad C_2 = \nu C_1, \quad C_3 = C_1/(1 + \mu_u/3K).$$

Here C_1 refers to the case (1.1), C_2 to (1.2), and C_3 to (1.6). It follows from (1.9) that if the shear modulus relaxes completely, then the background for the shear vibrations in the initial section will increase its growth $1 + \mu_u/3K$ times more intensively than for tension-compression vibrations. Moreover, the internal friction background ln tan δ depends linearly on 1/T in the initial section domain, and it is sufficient to measure the temperature dependences of tan δ for two excitation frequencies to determine U and γ.

It follows from (1.1), (1.2), and (1.6) that in the case $\gamma \neq 1$ saturation of the background should be observed at low frequencies while by virtue of the temperature-frequency equivalence and at high temperatures where the magnitude of the internal friction for tension-compression vibrations tends to the very same value as for shear vibrations, to the quantity tan ψ, and this limit value is independent of the moduli μ_u and K.

Let us estimate the magnitude of the temperature T_*, which conditionally separates the initial section domain of the background from its high-temperature (low-frequency) branch in which the saturation effect should be felt, for the case of tension-compression vibrations. By using the Arrhenius formula, we determine T_* as the temperature for which the components in the denominator of (1.6) are equal. The expression for T_* here has the form

$$T_* = \frac{\gamma U}{R}\left[\ln \frac{\cos(\pi\gamma/2)}{(1+\mu_u/3K)(\omega\tau_0)^\gamma}\right]^{-1}. \tag{1.10}$$

The deduction of saturation of the internal friction background had no reliable experimental confirmation for a long time. Data in agreement with the predicted effect were obtained for measurements of the frequency dependence of the background during torsional vibrations on an apparatus that permitted execution of investigations in the infralow frequency range to 10^{-5} Hz [3]. Background saturation was observed for values of the shear modulus comprising approximately half its unrelaxed value.

Moreover, experimental data on the temperature dependence of the internal friction background near the melting point are contradictory in nature. However, under repeated

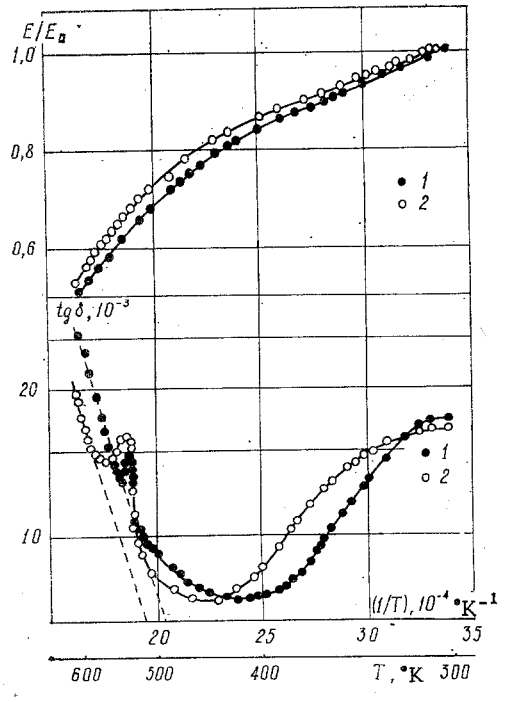

Fig. 1

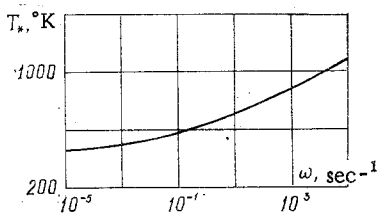

Fig. 2

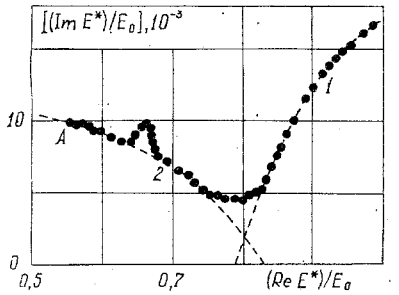

Fig. 3

annealings the plateau on the curve of the temperature dependence of the internal friction degenerated into a high-temperature maximum. On the other hand, no background saturation was observed during measurements on specimens of easily melting metals placed in an aluminum shell [5].

2. Results of an investigation of the internal friction of lead in the temperature range from room temperature to the melting point by methods of damped and forced bending vibrations of a vertically clamped foil are presented below. The experimental apparatus [6] assured measurement of the internal friction with less than 4% error, and the natural frequency with less than 0.2% up to the melting point. The amplitude of the relative deformation was $5 \cdot 10^{-6}$-$5 \cdot 10^{-7}$. Specimens in the form of 0.085-mm-thick foil were fabricated by rolling from the raw material C000. The specimens were annealed for one hour at a temperature of 585°K, which was 15°K below the melting point, in the apparatus directly before the measurements.

Displayed in Fig. 1 are graphs of ln tan δ and the relative Young's modulus E/E_0 proportional to the square of the natural vibrations frequency as a function of the reciprocal temperature. Here E_0 is the value of the Young's modulus at room temperature. The points 1 were obtained in measurements on a specimen with a 59-Hz natural vibrations frequency at room temperature, points 2 for 437 Hz. A domain of a high-temperature slope of the grain-boundary peak and a domain of a high-temperature branch of the background which is continued to the melting point can be separated out on the internal friction curves at temperatures from room to 420°K.

The maximum of the grain-boundary peak for measurements 2 on the specimen is at room temperature 296°K. The peak is broadened 2.6 times compared to the Debye value, i.e., is described by the relaxation time spectrum. A sharp drop in the Young's modulus corresponds to the domain of grain-boundary relaxation, where the domain of elastic modulus relaxation is narrower than the domain of the dissipative characteristic relaxation, tan δ. The activation energy of grain-boundary relaxation in lead, computed by means of the temperature shift of the slopes of the internal friction maximums of specimens 1 and 2, turned out to be $8.5 \cdot 10^4$ J/mole, which is 70% of the self-diffusion activation energy in lead [7].

The section of the high-temperature branch of the internal friction background is described by a linear dependence without saturation in a good approximation on a semilogarithmic scale. Values of the background activation energy and of the blurring parameter of the relaxation spectrum turned out to be $15 \cdot 10^4$ J/mole and 0.22. According to [8], the corresponding values for lead are $12 \cdot 10^4$ J/mole and 0.33. These quantities were obtained for measurements in the 0.45-2.0-Hz frequency band and the 373-513°K temperature range. The

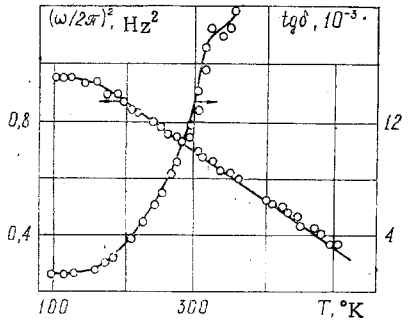

Fig. 4

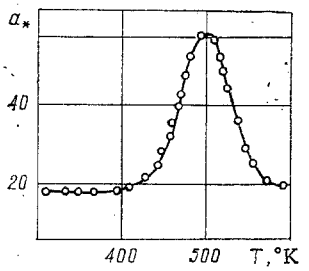

Fig. 5

difference observable can be explained by assuming that the specimen in [8] had initial plastic deformation and that the activation energy of the background diminished in this case while the blurring parameter of the relaxation spectrum increased, as is well established for the high temperature background of copper [6].

To estimate the frequency range in which the appearance of the background saturation effect could be expected, we consider the graph displayed in Fig. 2 for the dependence (1.10) of the temperature T_* on the cyclic frequency ω. The graph is constructed for the following values of the parameters (1.10): $\gamma = 0.22$, $U = 15 \cdot 10^4$ J/mole (experimental data), $\tau_0 = 10^{-13}$ sec [9], $\mu_u/3K = 0.125$ [10]. It is seen from Fig. 2 that the temperature T_* which equals the melting point of lead 600°K corresponds to the cyclic frequency $\omega \approx 10^{-1}$ sec^{-1}, i.e., the vibrations frequency ~10^{-2} Hz. In the resonance method being used the lower bound of the natural frequencies of specimen vibrations is ~10 Hz, while the frequency 10^{-2} Hz is unattainable. This explains the absence of the background saturation effect in Fig. 1.

It is also seen from Fig. 1 that high-temperature internal friction peaks are superposed on the rectilinear background sections in the 515-560°K temperature range. The maximums of these peaks are at 529 and 537°K, which is 0.88 and 0.90 of the melting point of lead. Such a maximum was observed at 0.94 of the melting point [5] in lead placed in an aluminum shell. The mechanism responsible for the origination of this maximum remains unclarified even yet.

Temperature dependences of the internal frication and elastic modulus are reconstructed in Re E*, Im E* coordinates in Fig. 3. Plotted along the axes are the quantities $(\mathrm{Re}\ E^*)/E_0 = (\omega/\omega_0)^2$ and $(\mathrm{Im}\ E^*)/E_0 = \tan\delta \cdot (\omega/_0)^2$, where ω_0 is the value of the cyclic frequency at room temperature. The diagram is a synthesis of two semicircles corresponding to grain-boundary relaxation (branch 1 of the diagram) and background (branch 2) with superposition of the high-temperature maximum on section 2. The extreme left point A of the diagram corresponds to the temperature 599°K of the specimen material, i.e., 1°K below the melting point. Measurement of the internal friction and elastic modulus values corresponding to the section of the diagram to the left of the point A was impossible because of the creep processes of the specimen material which developed intensively.

It is seen in Fig. 3 that the vector diagrams of the high-temperature relaxation processes in lead (background and grain-boundary relaxation) in the plane of the complex modulus have the form of circles (1.7) and are described well enough by the Maxwell generalized rheological models (1.3) and the standard linear body [1].

3. In connection with the fact that an exact determination of the values of the blurring parameters and the other characteristics of the relaxation spectrum from the vector diagrams is sufficiently complicated within the framework of the internal friction method, it is proposed to use a "quasi-resonance" method here to determine the same parameters [11].

The crux of the method is to measure the temperature dependence of the amplitude of the body vibrations when it is excited at the so-called "quasiresonance" frequency ω_*, which is determined completely in the linear case by the unrelaxation ω_u and relaxation ω_r frequencies of vibrations

$$\omega_* = \sqrt{\frac{\omega_u^2 + \omega_r^2}{2}}, \quad \frac{\omega_u^2}{\omega_r^2} = \frac{\mu_u}{\mu_r}. \tag{3.1}$$

Since at the melting point the Young's and shear moduli relax to zero, the expression (3.1) simplifies for the quasiresonance frequency to

$$\omega_* = \omega_u/\sqrt{2}. \tag{3.2}$$

Measurements of the background parameters by a quasiresonance method were carried out on an inverted torsional pendulum equipped with an infralow frequency generator in the 80-600°K range.

In order to determine the value of the quasiresonance frequency, the temperature dependence of the square of the system natural vibrations frequencies proportional to the shear modulus was found (Fig. 4). Also displayed in Fig. 4 is the temperature dependence of the tan δ of the specimens under investigation. A graph of the temperature dependence of the square of the natural vibrations frequencies has the shape of a broken line. The temperature of the beginning of the exponential dependence of the tangent of the mechanical loss angle corresponds to the temperature at which a break in the graph of the square of the natural vibrations frequencies is observed. The linear diminution in the elastic modulus in the 80-145°K temperature band is not related to any relaxation process, and is observed, in practice, down to the melting point for all crystalline materials. The steeper slope of the graph at temperatures above 145°K is explained by the superposition of the background effects. The value of the unrelaxed vibrations frequencies was determined by the break in the graph $\omega^2 = \omega^2(T)$ in Fig. 4 and $\omega_* = 4.33$ sec^{-1} was found from (3.2).

Intrinsically quasiresonance measurements were then performed. An alternating current voltage with frequency ω_* and constant amplitude was fed to the driving system of the apparatus, and the temperature dependence of the amplitude of the forced vibrations was measured. The data of the quasiresonance measurements are presented in Fig. 5. Values of the specimen vibrations amplitudes a_* at the quasiresonance frequency are indicated in relative units. The magnitude of the parameter γ was calculated from the formula [11]:

$$\gamma = \frac{4}{\pi} \operatorname{arc\,tg} \frac{a_{*1}}{a_{*2}},$$

where a_{*1} and a_{*2} are the minimal and maximal values of the specimen vibrations amplitudes, and turned out to equal 0.29, which is in good agreement with the data in [8].

The advantage of the quasiresonance method of determining the blurring parameter for the relaxation spectrum is its high accuracy, especially for a high level of system damping properties when different internal friction measures disclose a substantial difference in its behavior.

LITERATURE CITED

1. S. I. Meshkov, G. N. Pachevskaya, and T. D. Shermergor, "On the description of internal friction by using fractional-exponential kernels," Prikl. Mekh. Tekh. Fiz., No. 3 (1966).
2. S. I. Meshkov, Viscoelastic Properties of Materials [in Russian], Metallurgiya, Moscow (1974).
3. J. Woirgard and J. De. Fouquet, "High-temperature internal friction measured as a function of frequency between 10^{-5} Hz and 10 Hz on high purity metals," Proc. 6th Intern. Conf. on Internal Friction and Ultrasonic Attenuation in Solids, Tokyo (1977).
4. B. I. Shapoval, "On internal friction of metals at high temperatures," Fiz. Met. Metalloved., 18, No. 2 (1964).
5. B. M. Drapkin, A. A. Birfel'd, et al., "Study of Young's modulus and internal friction in the temperature range from 20°C to the melting point inclusive," Fiz. Met. Metalloved., 49, No. 5 (1980).
6. V. M. Guslikov, "Structure and internal friction of electrolytic copper sediments and the nucleus of composite materials on its basis," Candidate's Dissertation, Inst. Fiz. Akad. Nauk Gruz. SSR, Tbilisi (1981).
7. P. L. Gruzin, G. V. Kurdyumov, et al., "On the role of diffusion displacements of atoms in heat resistance," Investigations on Heat-Resistive Alloys [in Russian], Vol. 2, Izd. Akad. Nauk SSSR, Moscow (1957).
8. B. Ya. Pines and A. A. Karmazin, "On the question of the activation energy of the internal friction temperature background," Fiz. Met. Metalloved., 22, No. 4 (1966).
9. V. S. Postnikov, "Energy dissipation by a vibrating specimen at high temperatures," Fiz. Met. Metalloved., 7, No. 5 (1959).

10. T. Gorecki, "The relations between the shear modulus, the bulk modulus, and Young's modulus for polycrystalline metallic elements," Mater. Sci. Engng., 43, No. 3 (1980).
11. S. I. Meshkov, "Quasiresonance method of determining the relaxation spectrum parameters," Mechanisms of Relaxation Phenomena in Solids [in Russian], Nauka, Moscow (1972).

AXIALLY SYMMETRICAL COLLAPSE OF SPALLED LAYERS IN A CYLINDRICAL STEEL SHELL

A. G. Ivanov, V. N. Sofronov,
and E. S. Tyun'kin

UDC 539.415

There are several papers (see for example [1, 2] and bibliography there) on the spalling-free collapse of cylindrical shells as far as complete condensation. However, conditions frequently arise in explosion experiments that lead to spalling. Here we present results on the deformation and spalling in cylindrical steel shells on explosive loading, and we also give a theoretical description.

The loading intensity was such that the energy received by the shell was insufficient for complete collapse. We used shells made of St. 3 steel of outside diameter 47.6 mm, wall thickness 8.8 mm, and length 150 mm.

The loading was produced by a sliding detonation wave DW excited in a charge of TG 50/50 explosive placed directly on the outer surface. The DW was excited from one of the ends simultaneously around the circle by means of an explosive disk initiated at the center.

Figure 1 shows the shells after use. Table 1 gives the charge thicknesses Δ, the dimensions of the cross sections after loading (diameter and wall thickness), the thickness of the spalled layer, the shell strains ε, and the thickness of the spalled layer at the time of formation. The last was determined on the assumption that the layer arises by reflection of the first shock wave from the free boundary, when the displacement of the shell wall is slight (this assumption does not conflict with the calculations). The shell dimensions (Table 1) were obtained by averaging not less than 10 measurements.

The sections shown in Fig. 1 illustrate the effects of explosive layer thickness on the spalling damage as well as features of the spalled layer collapse. In all cases where the explosive thickness was less than the shell wall thickness, spalling occurred; spalling-free collapse occurred only in experiment 1 (Fig. 1a), where the explosive layer thickness was 10 mm.

In experiments 2 and 3 (Fig. 1b and c, explosive layer thicknesses respectively of 7.5 and 5 mm), the spalled layer collapsed stably without disintegration and became thicker by factors of 1.5 and 2.3 respectively, the strains being 35 and 38.5%.

On reducing the explosive thickness to 3 and 2 mm (Fig. 1d and e), the spalled layer broke up into fragments of size about 3 × 5 mm because of shear deformation and consequent loss of stable collapse. Finally, at a thickness of 1 mm (Fig. 1f) one gets the initial stage of spalling: A principal crack is generated and perturbations occur in the spalled layer. The strain in the remaining shell is also very much dependent on the charge thickness. When that thickness varies by a factor 10 (from 1 to 10 mm), ε varies by a factor 24 (from 0.84 to 20.4%), and the relationship is linear for charge thicknesses in the range 1-5 mm, but then there is a sharp increase accompanied by the occurrence of bending perturbations, which had the largest amplitude ($\Delta r/r \sim 3\%$) in experiment 2, where the deformation was quite large ($\varepsilon \sim 13.7\%$) and the thickness of the remaining shell was small. The number of perturbations in the shell was about 10, and the perturbations were not strictly periodic.

Moscow. Translated from Zhurnal Prikladnoi Mekhaniki i Tekhnicheskoi Fiziki, No. 3, pp. 125-127, May-June, 1984. Original article submitted April 15, 1983.

 0021-8944/84/2503-0452$08.50